JOURNAL OF AGRICULTURAL AND FOOD CHEMISTRY
ARTICLE

J. Agric. Food Chem. 2010, 58, 10169–10175 10169
DOI:10.1021/jf101943c

Species-Dependent Degradation of Ciprofloxacin in a Membrane Anodic Fenton System

Xiao Xiao, Xia Zeng, and Ann T. Lemley*

Graduate Field of Environmental Toxicology, FSAD, MVR Hall, Cornell University, Ithaca, New York 14853-4401

The anodic Fenton treatment method (AFT) has been successfully applied to the removal of ciprofloxacin (CIP), a widely used fluoroquinolone antibiotic, from aqueous solution. Degradation kinetics were found to be species dependent. At initial pH 3.2, CIP remained in its cationic form and the kinetics followed a previously developed AFT model. At an initial near-neutral pH, CIP speciation changed during the degradation, due to pH changes over the process, and no obvious model fit the data. Density functional theory (DFT) calculations indicated a protonated species-dependent reaction affinity toward hydroxyl radicals. A new model based on the AFT model with the addition of species distribution during the degradation was derived, and it was shown to describe the degradation kinetics successfully. Degradation of reference compounds further confirmed that the free carboxylic acid group, which contributes to the species changes, plays a key role in the observed degradation pattern. Furthermore, degradation of reference CIP−metal complexes confirmed that the formation of these complexes does not have a major effect on the degradation pattern. Optimization of CIP degradation was carried out at pH 3.2 with an optimal H_2O_2/Fe^{2+} ratio found between 10:1 and 15:1. Three degradation pathways based on mass spectrometry data were also proposed: (1) hydroxylation and defluorination on the aromatic ring; (2) oxidative decarboxylation; and (3) oxidation on the piperazine ring and dealkylation. By the end of the AFT treatment, neither CIP nor its degradation products were detected, indicating successful removal of antibacterial properties.

KEYWORDS: Ciprofloxacin; anodic Fenton treatment; DFT calculation; antibiotic; kinetic modeling; advanced oxidation

INTRODUCTION

On the basis of their annual global sales and therapeutic versatility, fluoroquinolones represent one of the most important classes of antibiotics (*1*, *2*). They are active against a wide spectrum of bacteria and are considered as "drugs of last resort". Ciprofloxacin (CIP) is one member of the second generation of fluoroquinolone derivatives. It is also a primary degradation product of enrofloxacin, another widely used fluoroquinolone drug. The structure of CIP is shown in **Figure 1**. CIP possesses a carboxylic acid group in the quinolone moiety (C-3, $pK_{a1} = 6.1$) and an amine group in the piperazine moiety (C-7, $pK_{a2} = 8.8$). Depending on the pH of the solution, CIP can exist as different species: anionic, cationic, or zwitterionic form. Speciation of CIP affects its sorption in soil, its photodegradation, and its reaction affinity toward ozone (*3*−*5*).

Antibiotics and their metabolites are ultimately discharged into wastewater treatment plants (WWTPs). However, there is a potential for releasing residual compounds into the aquatic environment within the treated effluents due to limited removal efficiency. In fact, CIP has been detected in WWTP effluents in the micrograms per liter concentration range and in the nanograms per liter concentration range in surface water after dilution (*6*, *7*). The presence and accumulation of fluoroquinolone antibiotics, even at low concentrations, may still pose threats to the ecosystem and human health by inducing the development and spread of drug resistance in bacteria due to long-term exposure. In addition, high concentrations of CIP, up to 31 mg/L, have been found in waste effluents from pharmaceutical manufacturers (*8*). In terms of precaution, it is necessary to explore effective treatment methods for removing contaminants before discharge.

Advanced oxidation processes (AOPs), characterized by hydroxyl radical generation, are attractive options for removing pharmaceuticals due to their capacity to rapidly and completely destroy organic compounds. One of the most employed and studied AOPs is the Fenton/Fenton-like system. Anodic Fenton treatment (AFT) has been developed in our laboratory and has shown great effectiveness in degrading organic pollutants (*9*, *10*). This treatment system is separated into two half-cells, which are connected by an anion exchange membrane. Sodium chloride is used as background electrolyte with a higher concentration in the cathodic cell.

The ferrous ion is delivered into the anodic half-cell via electrolysis of a sacrificial iron electrode, as shown in the following:

$$\text{anode}: \ Fe \rightarrow Fe^{2+} + 2e^- \quad (1)$$

$$\text{cathode}: \ 2H_2O + 2e^- \rightarrow H_2 + 2OH^- \quad (2)$$

*Corresponding author [phone (607) 255-3151; fax (607) 255-1093; e-mail atl2@cornell.edu.].

Published on Web 08/20/2010

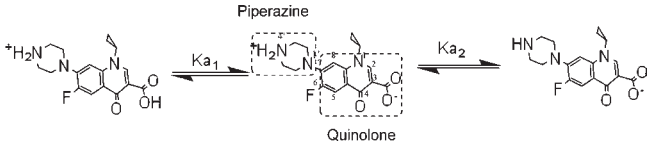

Figure 1. Speciation of CIP, $pK_{a1} = 6.1$, $pK_{a2} = 8.8$.

Hydrogen peroxide solution is pumped into the anodic half-cell to initiate the Fenton reaction.

$$\text{Fenton reaction}: \ Fe^{2+} + H_2O_2 \rightarrow Fe^{3+} + OH^- + OH\cdot \quad (3)$$

The concentration gradient of Cl^- in the two half-cells is beneficial for Cl^- to compete with OH^- in movement across the anion exchange membrane to the anodic cell, exerting less effect on the anodic pH and assisting in the development of an optimized acidic pH. A decrease of 3 pH units from the initial circum-neutral pH value has been observed (*11*).

The AFT kinetic model has been developed to simulate pollutant degradation in aqueous systems (*9*). Although the model has been successfully applied to several contaminants, it has not been tested for a compound with changing speciation during the AFT process. Because the pK_{a1} of CIP falls in the typical working pH range of AFT, species distribution will change due to pH changes during the process. In addition, in a Fenton system CIP may complex with the ferric ion. The extent of complex formation depends on solution pH and may affect the degradation process. The purpose of the present study is to (1) document the degradation of CIP in AFT, (2) determine the effect of pH-dependent speciation changes on the degradation process of CIP, (3) develop a kinetic model for CIP degradation, and (4) identify degradation products of CIP and propose degradation pathways in this system.

MATERIALS AND METHODS

Chemicals. All reagents were used without further purification. Ciprofloxacin (CIP) (98%), 1-phenylpiperazine (PP) (99%), and hydrogen peroxide (30%) were purchased from Sigma-Aldrich Chemicals (Milwaukee, WI). 1,6-dimethyl-4-oxo-1,4-dihydroquinoline-3-carboxylic acid (QA) (>95%) was purchased from Chembridge Corp. (San Diego, CA). All solutions were prepared from deionized water.

Anodic Fenton Treatment. The AFT apparatus consisted of two 400 mL glass half-cells separated by an anion exchange membrane (Electrosynthesis, Lancaster, NY). A scheme of the experimental apparatus was documented in a previous study (*12*). Typically, 200 mL of 55 μM CIP solution with 0.05 M NaCl was added into the anodic half-cell, and the same volume of 0.20 M NaCl aqueous solution was added into the cathodic half-cell. Each half-cell was stirred by a magnetic stir bar. Ferrous ion was generated by electrolysis in the anodic half-cell from a pure iron plate (0.5 cm × 10 cm × 0.2 cm) for the duration of the reaction. A graphite stick [1 cm (i.d.) × 10 cm (length)] was used as the cathode. The electrolysis current was controlled by a BK Precision DC power supply 1610 (TestPath, Inc., Danvers, MA). Hydrogen peroxide solution was delivered into the anodic half-cell using a STEPDOS diaphragm metering pump (KNF Neuberge Inc., Trenton, NJ) at a rate of 0.50 mL min^{-1} for the reaction period. The reaction was initiated by turning on the power supply when the first drop of hydrogen peroxide entered the solution in the anodic half-cell. Unless specified otherwise, electric current was kept at 0.040 A, with a Fe^{2+}:H_2O_2 delivery ratio of 1:10, and all experiments were conducted at room temperature, 24 ± 1 °C. One milliliter of sample was collected (by an Eppendorf pipet) from the anodic cell at 20 s intervals in the first 2 min and at 30 s intervals for the final 3 min. The sample was transferred to a 2 mL HPLC vial containing 0.1 mL of methanol, which quenches hydroxyl radicals. Each treatment was done with three replicates. AFT degradation of CIP−metal complexes (CIP−Al, CIP−Fe) and reference compounds was conducted similarly. CIP−Al and CIP−Fe complexes were synthesized by the addition of excess metal ions into the CIP solution at pH ~4. The methyl ester of CIP (CIPME) was synthesized in methanol catalyzed by concentrated sulfuric acid with 4 h of refluxing and was confirmed by mass spectrometry. Esterification of the reference compound QA was conducted similarly. The pH was adjusted to the desired level before the anodic Fenton treatment.

Analytical Methods. The concentrations of CIP, reference compounds, and their degradation products were analyzed by a reverse-phase high-performance liquid chromatograph (HPLC) with a diode array UV−vis detector (HP series 1200, Agilent Technology) and a Restek ultra C18 (5 μm) reverse phase column (4.6 × 150 mm) thermostated at 25 °C. The detector wavelength was set at 230−280 nm. Gradient elution was used with the mobile phase containing 0.1% formic acid (eluent A) and acetonitrile (eluent B). The eluent A/eluent B ratio was changed from 95:5 to 45:55 over 12 min, from 45:55 back to 95:5 over 2 min, and remained at 95:5 for the last minute. Degradation products were analyzed by an Agilent G1978B Multimode source for the 6100 series single-quadropole MS in the positive ES mode with a full scan from m/z 50 to m/z 700 and a fragmentor of 180. The specific parameters set up for the mass detector was as follows: drying gas flow, 12 L min^{-1}; nebulizer pressure, 40 Psig; drying gas temperature, 300 °C; vaporizer temperature, 250 °C; capillary voltage, 2000 V; corona current, 4.0 μA; and charging voltage, 2000 V.

Kinetic Modeling. The derivation of the AFT kinetic model was established in a previous paper (*9*). The degradation kinetics of the target organic compound can be described by the equation

$$\ln \frac{[C]_t}{[C]_0} = \frac{1}{2} K\lambda\pi\omega v_0^2 t^2 \quad (4)$$

where $K = kk_1$ (μM^{-2} min^{-2}), k (μM^{-1} min^{-1}), and k_1 (μM^{-1} min^{-1}) are the second-order rate constants of the Fenton reaction and the reaction between hydroxyl radical and target compound, respectively; $[C]_0$ (μM) and $[C]_t$ (μM) are the concentrations of the target compound at 0 and t min, respectively; λ (min) and π (min) are the average lifetimes of the hydroxyl radical and the ferrous ion, respectively; ω is a constant related to the delivery ratio of hydrogen peroxide to ferrous ion and to the consumption ratio of hydrogen peroxide; v_0 (μM min^{-1}) is the delivery rate of ferrous ion by electrolysis; and t (min) is time.

Density Functional Theory (DFT) Calculation. The hybrid method B3LYP with the standard 6-31G (d) basis set was used to calculate the potential energies of the compounds involved during the reaction of CIP and hydroxyl radicals (Gaussian 03 software). All structures involved in the reaction were located on the potential energy surface by performing full geometry optimization, and their natures were identified by performing frequency calculations.

RESULTS AND DISCUSSION

Degradation of CIP at Different Initial pH Values. CIP was degraded at two different initial pH conditions, 3.2 and 6.2−6.8. These two pH ranges were chosen for several reasons. The acidic pH (3.2) is a favorable condition for the Fenton reaction, and it is also an unfavorable condition for complex formation between CIP and ferric ion. Thus, CIP should exist mainly in the cationic form. The pH range of 6.2−6.8 is near the pK_{a1} of CIP. With this starting pH, CIP species ratios will change continuously during the self-acidifying AFT process. This range also gives pH values similar to the natural environment. Over the pH range of this study, the piperazinyl 4′-*N*, which corresponds to pK_{a2}, remains protonated. Thus, we refer to protonated or deprotonated CIP according to the speciation of the carboxylic acid group (**Figure 1**).

AFT treatment worked efficiently to remove CIP at both pH conditions; a total removal was observed within 4 min (**Figure 2**). CIP degradation showed different patterns at different initial pH values. At initial pH 3.2, the solution pH remained almost stable during the process and the AFT model fitted the degradation kinetics well with $R^2 > 0.99$. At initial pH 6.2−6.8, the solution pH changed from above 6 to around 3.7. The degradation data deviated from a typical AFT-type curve with a much faster degradation in the first minute. Neither a first-order kinetic model, the AFT model, nor the modified AFT model gave a good fit to the data at this initial pH. (The modified model accounts for a weak interaction

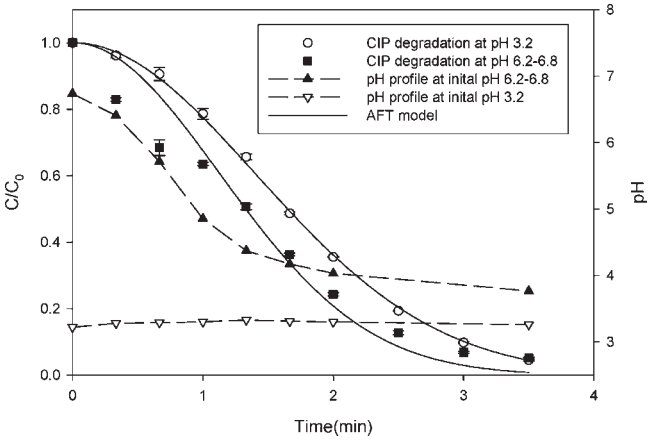

Figure 2. Degradation of CIP in AFT system at pH_0 3.2 and 6.2−6.8. Current delivery = 0.04A; $[H_2O_2]/[Fe^{2+}]$ = 10:1; $[CIP]_0$ = 55 μM.

between the ferric ion and a heterocyclic nitrogen. See the Supporting Information for a further description of the modified model.)

Degradation of Reference Compounds. To confirm the role of the carboxylic acid functional group in the degradation kinetics observed at the initial pH of 6.2−6.8, a series of reference compounds, PP, QA, and CIPME, were studied with AFT, similar to the CIP experiments (Figure S1). These compounds were chosen to represent the two structural parts of CIP, which correspond to the two protonation sites, also susceptible sites for ozonation and hydroxyl radical attack (*13*). The reference compound PP has a piperazinyl substituent on the benzene ring, and reference compound QA maintains the quinolone core structure. CIPME was synthesized via methylation of the carboxylic acid. CIPME and PP exist only in the cationic form, whereas QA speciation changes with pH changes during the AFT process.

AFT effectively degraded all of the reference compounds, although different kinetic patterns were observed. At pH 3.2, all of the compounds followed the AFT model, indicating that the model worked well for this optimized, simplified condition (Figure S2). At pH 6.2−6.8, the degradation kinetics of PP and CIPME followed the modified AFT model, indicating a weak interaction between the probe chemicals and iron, possibly via the heterocyclic nitrogen. The degradation profile of QA gave an interesting curve that looks similar to CIP-type kinetics at the initial pH, although subtler during the first minute (Figure S3).

The results indicate that the carboxylic acid group may play a key role in the kinetics of degradation, because absence of this functional group (as in PP) and methylation of CIP gave different degradation patterns. In contrast, QA, a structural analogue with a free carboxylic acid, followed a degradation pattern similar to that of CIP. To further confirm the role of carboxylic acid on the quinolone structure, QA was esterified and degraded by AFT. The degradation kinetics shifted from a CIP-type curve to a typical AFT curve, further supporting the essential role of the free carboxylic acid group (Figure S3).

In addition to protonation at the acidic pH, the carboxylic acid group may complex with iron easily when it is in a deprotonated form at a higher pH. Thus, two hypotheses were proposed as to how the carboxylic acid group might affect the degradation kinetics: (I) CIP undergoes protonation during the treatment, leading to a change in distribution of CIP species, which have different reactivities with hydroxyl radicals, and the resulting degradation pattern is a hybrid of the two kinetic degradation patterns, one from each species. (II) CIP may complex with iron at near-neutral initial pH, and this complex formation may affect either the Fenton reaction or the CIP reaction affinity

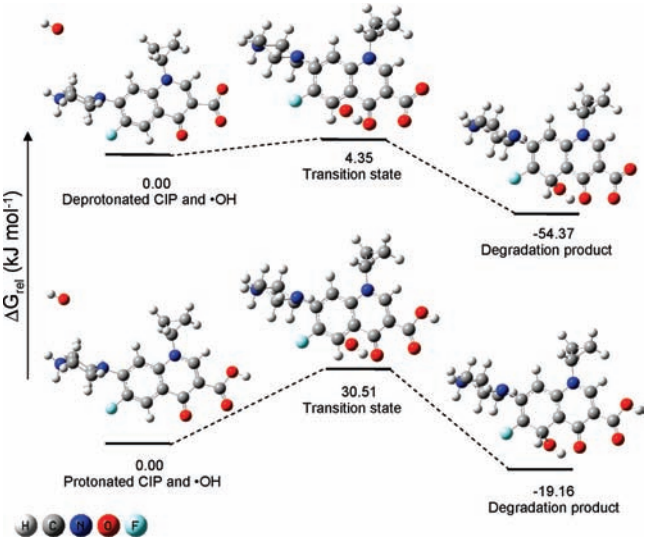

Figure 3. Calculated potential energy surface profiles for reactions between deprotonated and protonated CIP with hydroxyl radical by Gaussian 03 (B3LYP/6-31G).

toward the OH radical, resulting in a shift in kinetics during the first minute.

CIP Protonation/Deprotonation Effect on Degradation. A buffer system at neutral pH, which assists in maintaining CIP speciation, cannot be used in the AFT system due to strong interference with the Fenton reaction. To test the first hypothesis of speciation-dependent reactivity of CIP with hydroxyl radicals due to protonation, DFT calculations of potential energies during the reaction were carried out. Because the change in kinetics took place during the first minute, it was assumed that the first major reaction determined the kinetic pattern. On the basis of the mass spectrometric data of the CIP degradation products, the first reaction is hydroxyl addition to the aromatic ring. Therefore, the potential energy surface profiles of CIP, the hydroxyl radical, and 5-hydroxylated CIP were calculated and are shown in **Figure 3**. For the deprotonated CIP and OH radical, a lower transition state energy was found compared to that of protonated CIP, with a significant energy difference of 26.16 kJ mol^{-1} for the transition states. An observable difference in reaction rates is expected, supporting our first hypothesis that the difference in reaction affinity of the different CIP species with hydroxyl radicals is an explanation for the kinetic degradation pattern. This result is consistent with the hydroxyl radical being a strong electrophile with greater affinity for and reactivity with the neutral deprotonated CIP than the positively charged protonated CIP.

CIP−Metal Complex Effect on Degradation. Another possible cause for the change in kinetics is the complex formation between CIP, a carboxylate Lewis base, and iron, a strong Lewis acid. Various studies have shown the formation of CIP−metal complexes, most likely in a bidentate mode via the 3-carboxylate and 4-carbonyl groups (*14*, *15*). The complex formation between metal ions and fluoroquinolones depends on pH due to the competition between polyvalent ions and protons (*16*).

To investigate the complex formation hypothesis, AFT was carried out on a CIP−Al complex and on a CIP−Fe complex (**Figure 4**). Because Al has a CIP binding affinity similar to that of the ferric ion, preaddition of excess Al ion before AFT should cause the formation of a CIP−Al complex and minimize CIP−ferric complex formation. Degradation data of the CIP−Al complex at pH 6.2−6.8 overlapped with that of CIP during the first minute, indicating a negligible effect of this complex on the Fenton reaction. There is a slower degradation of CIP−Al after 1.5 min, with the remainder of the degradation pattern appearing to follow a

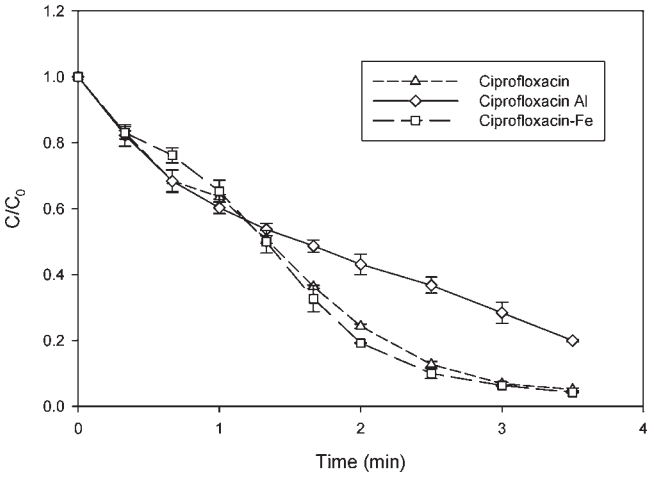

Figure 4. Degradation of CIP and CIP−metal complex with current delivery = 0.04 A; initial pH 6.2−6.8; $[H_2O_2]$:$[Fe^{2+}]$ = 10:1; and $[CIP]_0$, $[CIP\text{-}Al]_0$, $[CIP\text{-}Fe]_0$ = 55 μM.

first-order curve. This phenomenon might be due to the buffering capacity of $Al(OH)_4^-$ at the starting pH, thus preventing a shift to the ideal, lower pH for Fenton systems and a consequent slowing of the reaction (Figure S4) (*17*). The pH buffering effect of humic acid that slows degradation was observed in a previous study, in which a similar first-order like curve was found (*18*).

To further test how complex formation affects reaction affinity of CIP toward the hydroxyl radical, AFT was run in a system with preaddition of excess ferric ion, thus causing formation of a CIP−ferric complex before AFT treatment. If the complex has a major effect on the reaction affinity of CIP, we would expect to see a change in the degradation curve, especially during the first minute because this is the critical period when ferric ion accumulates (from oxidation of ferrous ion) and begins to bind with CIP. Interestingly, a degradation pattern similar to that of CIP was observed, indicating no effect of excess ferric ion on CIP degradation.

On the basis of the degradation kinetics of both CIP−metal complexes, it can be concluded that the complex formation with metal ion is too weak to cause effects, if any, on the degradation kinetics. Therefore, the observed kinetics are caused by protonation/deprotonation, generating two species of CIP that react differently with OH radicals.

Development of the AFT′ Model. A model based on the protonation/deprotonation hypothesis (the AFT′ model) was developed that accounts for the change of species distribution during degradation. The goal was not to develop a generalized model but to simulate the CIP degradation in the AFT system. Successful model fitting further provides a confirmation of the hypothesis.

The pH was monitored throughout the degradation (Figure S5), and a distribution of CIP species was calculated according to the following acid−base equilibrium and Henderson−Hasselbalch equation.

$$HCIP^+ \Leftrightarrow CIP + H^+ \tag{5}$$

$$\frac{[CIP]}{[HCIP^+]} = \frac{10^{-pKa}}{10^{-pH}} = \text{ratio} \tag{6}$$

$$CIP\% = \frac{CIP}{CIP + HCIP^+} \times 100\% = \frac{\text{ratio}}{\text{ratio} + 1} \tag{7}$$

Species distribution curves were obtained by plotting the percentage of deprotonated CIP as a function of time (Figure S6). Of several mathematical models tried, the Gaussian model provided the best fit for the distribution curves ($R^2 > 0.98$). This function can be represented by

$$CIP\% = a + c\exp(-bt^2) \tag{8}$$

where t is reaction time and a, b, and c are coefficients used in the Gaussian model.

Assuming each species has a different reaction rate with the hydroxyl radical and each species follows the AFT model, that is, both the Fenton reaction and the reaction between the CIP species and hydroxyl radicals follow second-order kinetics, a new model can be derived, which we call the AFT′ model:

$$\frac{C}{C_0} = \exp\left(\frac{-Kk_1'}{2} \times \left(at^2 - \frac{c}{b}\exp(-bt^2)\right) - \frac{Kk_2'}{2} \times \left(\frac{c}{b}\exp(-bt^2) - (a-1)t^2\right) - \frac{c}{b} \times \left(\frac{Kk_2'}{2} - \frac{Kk_1'}{2}\right)\right) \tag{9}$$

$K = k\lambda\pi\omega{v_o}^2$, and k'_1 and k'_2 are the second-order reaction rate constants of deprotonated and protonated CIP with hydroxyl radicals, respectively.

To test the validity of the AFT′ model, concentration profiles of CIP degradation at various currents (iron delivery rates) at initial pH 6.2−6.8 were fitted (**Figure 5A**). Compared to the previous AFT model ($R^2 \sim 0.9$), the AFT′ model showed a major improvement in describing the kinetics ($R^2 > 0.97$, **Figure 5B**). The AFT′ model worked best for degradation at the higher Fenton reagent delivery rates (≥0.04 A). At lower delivery rates, the model cannot capture the changes of CIP concentration well in the first few seconds. This observation may indicate a larger error in estimating distribution of CIP species at lower iron deliveries or other complicating factors that may need to be taken into consideration.

Optimization of CIP Degradation. The experimental conditions of CIP degradation by AFT were optimized at pH 3.2. A series of experiments were carried out with various Fenton reagent delivery rates, H_2O_2:Fe^{2+} ratios, and initial CIP concentrations. All degradation kinetics followed the AFT model. The degradation rate was faster with increased Fenton reagent delivery rates, where a faster generation of hydroxyl radicals would be expected, and slower with increased initial CIP concentration (Figures S7 and S8).

Due to hydroxyl radical quenching by iron and hydrogen peroxide, the ratio of ferrous ion to hydrogen peroxide is seldom stoichiometric. An optimal ratio between 10 and 15 was found, consistent with previous results that showed an optimal ratio of 11 (Figure S9) (*9*).

CIP Degradation Product Analysis and Proposed Pathways. Degradation products obtained at two initial pH conditions were analyzed by HPLC-MS. Due to the instrumentation used and the difficulty of obtaining pure standards, the MS results obtained in this study provide preliminary results for possible degradation pathways of CIP in the AFT system. Representative chromatograms are given in the Supporting Information (Figures S10 and S11). Degradation mixtures at 2.5 min at both conditions were chosen for analysis due to the relatively high concentrations of major products. The products were analyzed by identifying the $[M + H]^+$ molecular ions in the positive mode. Four major peaks with molecular ions of m/z 348, 362, 330, and 263 were found at both pH values, although slight differences in degradation pattern were observed. A trace amount of m/z 334 was seen at neutral condition, whereas a much higher concentration of m/z 334 was detected at acidic condition. This observation may indicate a species-dependent preference in pathways. In addition, a different pathway may occur with a neutral

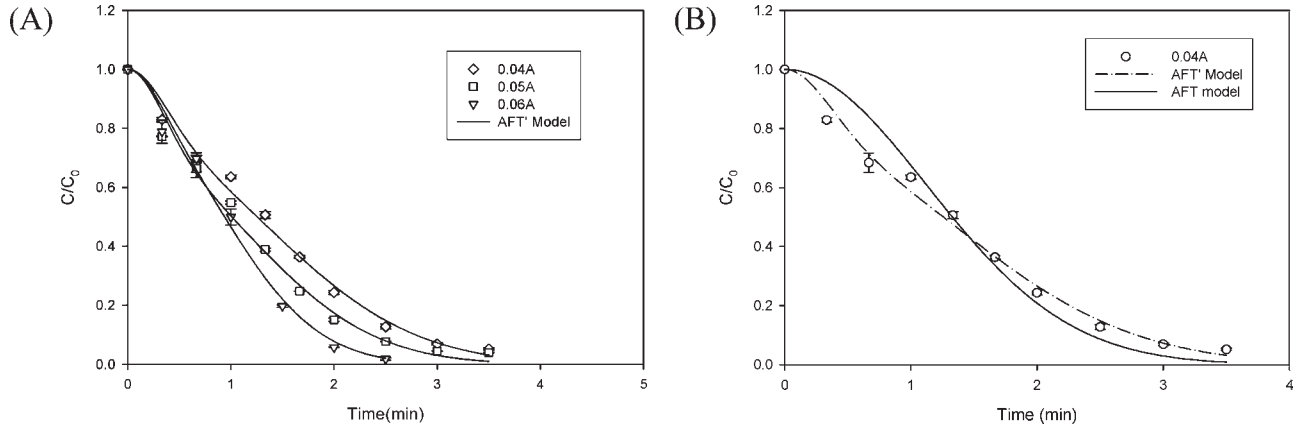

Figure 5. (**A**) Degradation of CIP with current delivery = 0.04−0.06 A, $[H_2O_2]$:$[Fe^{2+}]$ = 10:1, initial pH 6.2−6.8; and $[CIP]_0$ = 55 μM. The data were fitted by the AFT′ model. (**B**) Comparison of AFT model and AFT′ model by fitting degradation data at current delivery = 0.04 A.

initial pH because the peak with a molecular ion of *m*/*z* 328 was detected only at this condition. Several minor products were also observed at both pH conditions, including *m*/*z* 291, *m*/*z* 304, *m*/*z* 302, and *m*/*z* 261. Due to their low concentrations, it is hard to determine if the degradation products were preferentially formed at a given pH. The fragmentation patterns of products were also compared with those reported in the literature. Several similar products have been found in previous studies, in which CIP was oxidized by various methods (*19*−*21*). The mass spectrum profiles of the peaks are summarized in **Table 1**, and proposed pathways are shown in **Figure 6**.

The aromatic ring of CIP has been observed to be a susceptible site for hydroxylation (*21*, *22*); thus, *m*/*z* 348 is proposed to be the product of such hydroxylation. The reaction can take place at C-5 or C-8. Under the LC conditions used, the two products cannot be separated efficiently, and a mixture is expected. The observed fast formation of *m*/*z* 348 supports hydroxyl addition on the aromatic ring, a well-known fast reaction (*22*). Another well-known degradation pathway is defluorination (*13*, *21*, *22*). During defluorination, the attack of the hydroxyl radical at the carbon−fluorine position leads to a geminal fluorohydrin intermediate that undergoes HF elimination. The *m*/*z* 330 product is suggested as consistent with this pathway. Multiple hydroxylations are also likely to happen, which may explain the formation of *m*/*z* 362. Its relatively late formation time also supports this multiple-step reaction pathway (**Figure 7**).

Previous studies on CIP degradation suggest that the piperazinyl substituent is a likely susceptible site to hydroxyl radical attack (*13*, *20*, *21*, *23*). The *m*/*z* 263 species is proposed to form via the complete dealkylation of the piperazine ring. A trace amount of *m*/*z* 261 was also observed. This compound may be formed via a pathway similar to that of *m*/*z* 263, except for a further defluorination step. The *m*/*z* 263 and *m*/*z*261 species were the final products observed, which is consistent with their late formation time (**Figure 7**). Intermediates of dealkylation reported in other studies, such as desethylene CIP, were not observed. This result may be due to a short half-life or very low concentration of the intermediates in AFT. The *m*/*z* 334 and *m*/*z* 291 species are suggested to be upstream products of *m*/*z* 263, which are derived from oxidation of the piperazine ring of CIP. Two *m*/*z* 334 isomers were observed with a large difference in LC retention time. This may be explained by the different polarities of the secondary and tertiary amines.

The *m*/*z* 328 species has not been reported before. It may be formed by OH radical attack at both the piperazine ring and the C-6 of the quinolone ring, resulting in a C=N double-bond formation in the piperazine ring and defluorination on the quinolone core (*24*). Oxidative decarboxylation is also a likely mechanism for degradation of CIP, although it occurs to a lesser extent. This pathway may account for the trace amounts of *m*/*z* 302 and *m*/*z* 304 observed.

Table 1. Mass Spectrum Profiles of Peaks for CIP Degradation Intermediates

pseudomolecular ion (M + H$^+$)	mass spectrum profile[a]	retention time (min)	observed reaction system pH
332	354(29), 332(83), 314(32), 288(1.2) (CIP)	9.46	
263	285(13), 263(39), 245(100)	13.49	both
348	370(31), 348(54), 330(85)	9.01	both
330	352(33), 330(65), 312(24)	8.22	both
304	326(4), 304(15), 286(14)	7.619	both
302	302(16)	7.811	both
362	384(61), 362(100), 344(51)	8.53	both
334(1)	356(26), 334(64), 316(57)	8.73	mainly acidic
334(2)	356(17), 334(78), 316(41)	12.34	mainly acidic
291	291(20), 273(56)	13.063	acidic
328	350(11), 328(69), 310(32)	8.682	neutral

[a] Mass spectrum profile is a summary of the fragments observed for each product.

It is believed that destruction of piperazinyl substituents only partially removes the antibiotic activity of CIP (*25*). Also, most of the modifications on the quinolone ring observed here cannot alter the antibiotic properties to a great extent because the structures still share considerable similarity to CIP (*26*). Therefore, we monitored the CIP reaction mixtures during the entire process to study the evolution of the products (only primary products are shown in **Figure 7**). All of the peak areas show an increase in area (qualitatively correlated with concentration) followed by a general trend toward decrease in area at 3−5 min. By the end of the treatment, not only was CIP completely removed, but the degradation products were degraded to below the LC-MS detection limit, indicating successful removal of antibacterial intermediates. Ciprofloxacin is resistant to biodegradation, due to its antibiotic nature (*27*). Sorption is the major removal mechanism in wastewater treatment plants, leading to a potential release to the soil environment if the sludge is used as a soil amendment/fertilizer (*28*). The AFT system shows an efficient oxidation of CIP and its antibacterial intermediates and can be a promising technology to treat such wastewater.

ABBREVIATIONS USED

AFT, anodic Fenton treatment; CIP, ciprofloxacin; PP, 1-phenylpiperazine; QA, 1,6-dimethyl-4-oxo-1,4-dihydroquinoline-3-carboxylic acid; CIPME, methyl ester of ciprofloxacin; DFT,

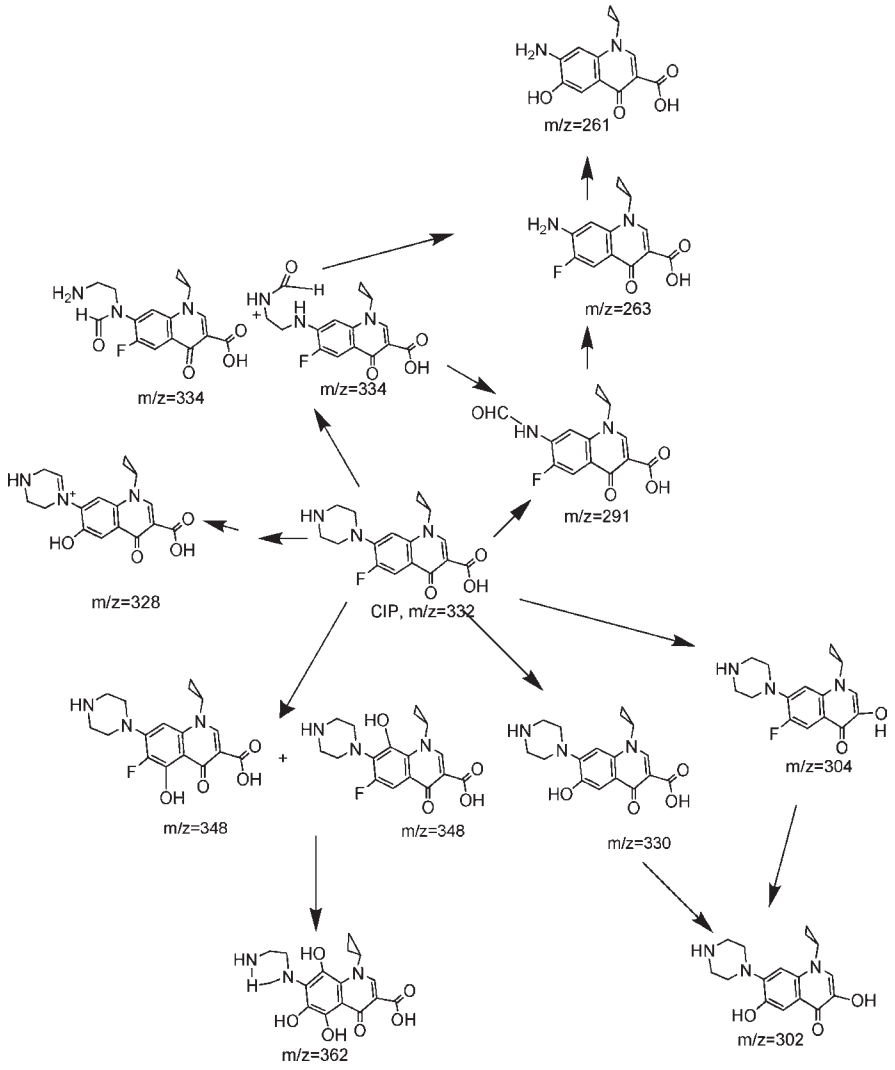

Figure 6. Proposed degradation pathways of CIP in the AFT system.

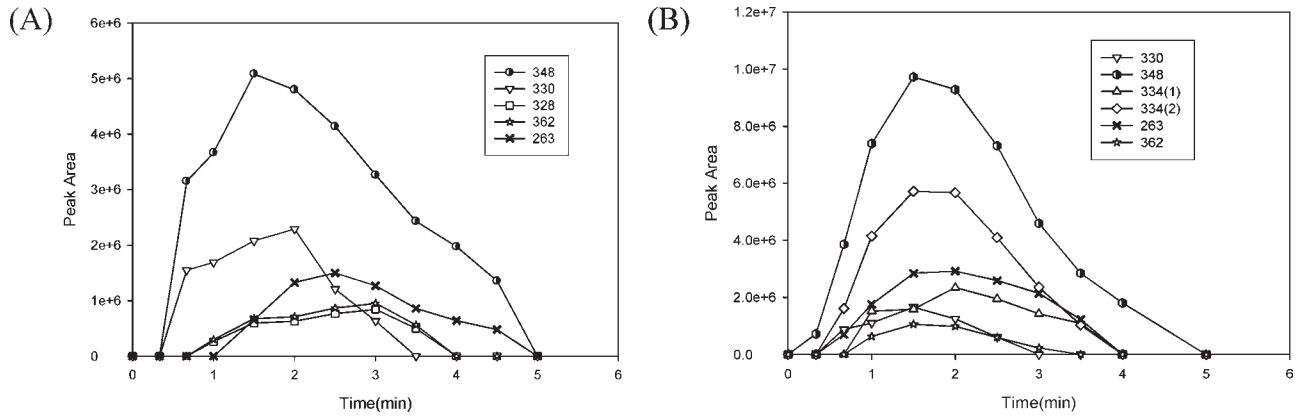

Figure 7. Evolution of CIP degradation products: (**A**) initial pH 6.2−6.8; (**B**) initial pH 3.2. Current delivery = 0.04 A; $[H_2O_2]$:$[Fe^{2+}]$ = 10:1; [CIP] = 55 μM. Peak areas are from total ion chromatogram.

density functional theory; HPLC, high-performance liquid chromatography; LC-MS; liquid chromatography−mass spectrometry; WWTP, wastewater treatment plants; AOPs, advanced oxidation processes.

Supporting Information Available: Structures of reference compounds; degradation of reference compounds in the AFT system; pH profiles during degradation of CIP and CIP−metal complexes; percentage of deprotonated CIP during the AFT process; degradation of CIP at initial pH 3.2 with various delivery rates, initial concentrations, H_2O_2/Fe^{2+} ratios; representative chromatograms of CIP degradation products at two different initial pH conditions; description of modified AFT model and derivatization of AFT′ model. This material is available free of charge via the Internet at http://pubs.acs.org.

LITERATURE CITED

(1) Dodd, M. C.; Shah, A. D.; Gunten, U. V.; Huang, U. C.-H. Interactions of fluoroquinolone antibacterial agents with aqueous chlorine: reaction kinetics, mechanisms, and transformation pathways. *Environ. Sci. Technol.* **2005**, *39*, 7065–7076.

(2) Picó, Y.; Vicente, A. Fluoroquiolones in soil − risks and challenges. *Anal. Bioanal. Chem.* **2007**, *387*, 1287–1299.

(3) Gu, C.; Karthikeyan, K. G. Sorption of antimicrobial CIP to aluminum and iron hydrous oxides. *Environ. Sci. Technol.* **2005**, *39*, 9166–9173.

(4) Torniainen, K.; Tammilehto, S.; Ulvi, V. The effect of pH, buffer type and drug concentration on the photodegradation of CIP. *Int. J. Pharm.* **1996**, *132*, 53–61.

(5) Dodd, M. C.; Buffle, M. O.; Gunten, U. V. Oxidation of antibacterial molecules by aqueous ozone: moiety-specific reaction kinetics and application to ozone-based wastewater treatment. *Environ. Sci. Technol.* **2006**, *40*, 1969–1977.

(6) Kolpin, D. W.; Furlong, E. T.; Meyer, M. T.; Thurman, E. M.; Zaugg, S. D.; Barber, L. B.; Buxton, H. T. Pharmaceuticals, hormones, and other organic wastewater contaminants in U.S. streams, 1999−2000: a national reconnaissance. *Environ. Sci. Technol.* **2002**, *36*, 1201–1211.

(7) Gros, M.; Petrovic, M.; Barcelo, D. Tracing pharmaceutical residues of different therapeutic classes in environmental waters by using liquid chromatography/quadrupole-linear ion trap mass spectrometry and automated library searching. *Anal. Chem.* **2009**, *81*, 898–912.

(8) Larsson, D. G.; De Pedro, C.; Paxeus, N. Effluent from drug manufactures contains extremely high levels of pharmaceuticals. *J. Hazard. Mater.* **2007**, *148*, 751–755.

(9) Wang, Q.; Lemley, A. T. Kinetic model and optimization of 2,4-D degradation by anodic Fenton treatment. *Environ. Sci. Technol.* **2001**, *35*, 4509–4514.

(10) Neafsey, K.; Zeng, X.; Lemley, A. T. Degradation of sulfonamides in aqueous solution by membrane anodic Fenton treatment. *J. Agric. Food Chem.* **2010**, *58*, 1068–1076.

(11) Saltmiras, D. A.; Lemley, A. T. Atrazine degradation by anodic Fenton treatment. *Water Res.* **2002**, *36*, 5113–5119.

(12) Wang, Q.; Lemley, A. T. Oxidation of carbaryl in aqueous solution by membrane anodic Fenton treatment. *J. Agric. Food Chem.* **2002**, *50*, 2331–2337.

(13) Dewitte, B.; Dewulf, J.; Demeestere, K.; Vyvere, V.; Wispelaere, P.; Langenhove, H. Ozonation of CIP in water: HRMS identification of reaction products and pathways. *Environ. Sci. Technol.* **2008**, *42*, 4889–4895.

(14) Trivedi, P.; Vasudevan, D. Spectroscopic investigation of CIP speciation at the goethite−water interface. *Environ. Sci. Technol.* **2007**, *41*, 3153–3158.

(15) Djurdjević, P.; Stankov, M. J.; Odović, J. Study of solution equilibria between iron(III) ion and CIP in pure nitrate ionic medium and micellar medium. *Polyhedron* **2000**, *19*, 1085–1096.

(16) Walls, S. C.; Charles, B. G.; Gahan, L. R.; Filippich, L. J.; Bredhauer, M. G.; Duckworth, P. A. Interaction of norfloxacin with divalent and trivalent pharmaceutical cations. In vitro complexation and in vivo pharmacokinetic studies in the dog. *J. Pharm. Sci.* **1996**, *85*, 803–809.

(17) Pignatello, J. J. Advanced oxidation processes for organic contaminant destruction based on the Fenton reaction and related chemistry. *Environ. Sci. Technol.* **2006**, *36*, 1–84.

(18) Wang, Q. Q.; Lemley, A. T. Kinetic effect of humic acid on alachlor degradation by anodic Fenton treatment. *J. Environ. Qual.* **2004**, *33*, 2343–2352.

(19) Calza, P.; Medana, C.; Carbone, F.; Giancotti, V.; Baiocchi, C. Characterization of intermediate compounds formed upon photo-induced degradation of quinolones by high-performance liquid chromatography/high resolution multiple-stage mass spectrometry. *Rapid Commun. Mass Spectrom.* **2008**, *22*, 1533–1552.

(20) Zhang, H. C.; Huang, C. H. Oxidative transformation of fluoroquinolone antibacterial agents and structurally related amines by manganese oxide. *Environ. Sci. Technol.* **2005**, *39*, 4474–4483.

(21) Wetzstein, H. G.; Stadler, M.; Tichy, H. V.; Dalhoff, A.; Karl, W. Degradation of CIP by basidiomycetes and identification metabolites generated by the brown rot fungus *Gloeophyllum striatum*. *Appl. Environ. Microbiol.* **1999**, *65*, 1556–1563.

(22) Santoke, H.; Song, W.; Cooper, W. J.; Greaves, J.; Miller, G. E. Free-radical-induced oxidative and reductive degradation of fluoroquinolone pharmaceuticals: kinetic studies and degradation mechanism. *J. Phys. Chem. A* **2009**, *113*, 7846–7851.

(23) Wetzstein, H.; Schneider, J.; Karl, W. Patterns of metabolites produced from the fluoroquinolone enrofloxacin by basidiomycetes indigenous to agricultural sites. *Appl. Mcirobiol. Biotechnol.* **2006**, *71*, 90–100.

(24) Surdhar, P. S.; Armstrong, D. A. Reactions of α-carbon- and nitrogen-centered radicals of piperazine with lumiflavin and para-nitroacetophenone at pH 7. *Can. J. Chem.* **1988**, *66*, 535–540.

(25) Vasconcelos, T. G.; Henriques, D. M.; König, A.; Martins, A. F.; Kümmerer, K. Photo-degradation of the antimicrobial CIP at high pH: identification and biodegradability assessment of the primary by-products. *Chemosphere* **2009**, *76*, 487–493.

(26) Jjemba, P.; Robertson, B. Antimicrobial agents with improved clinical efficacy versus their persistence in the environment: synthetic 4-quinolone as an example. *Ecohealth* **2005**, *2*, 171–182.

(27) Kümmerer, K.; Al-Ahmad, A.; Mersch-Sundermann, V. Biodegradability of some antibiotics, elimination of the genotoxicity and affection of wastewater bacteria in a simple test. *Chemosphere* **2000**, *40*, 701–710.

(28) Golet, E.; Xifra, I.; Alder, A.; Giger, W. Environmental exposure assessment of fluoroquinolone antibacterial agents from sewage to soil. *Environ. Sci. Technol.* **2003**, *37*, 3243–3249.

Received for review May 20, 2010. Revised manuscript received August 5, 2010. Accepted August 09, 2010. This study was funded in part by the College of Human Ecology, Cornell University, and in part by the Cornell University Agricultural Experiment Station federal formula funds, Project NYC-329806 (W-1045), received from the Cooperative State Research, Education, and Extension Service, U.S. Department of Agriculture. Any opinions, findings, conclusions, or recommendations expressed in this publication are those of the author(s) and do not necessarily reflect the views of the U.S. Department of Agriculture.